Phase Visualization Using Modified Llyod Mirror Interferometer

Amit Kumar Sharma[1]*,Roopesh Kumar[2]

[1]Department of Physics, D.A.V. (PG) College, Dehradun
*E-mail: aoemit@rediffmail.com

[2]Department of Physics D.B.S (PG) College, Dehradun

Abstract

Llyod Mirror interferometers are though quite suitable to carry out study on phase objects in finite-fringe mode but in its present form it is difficult to work with this interferometer in infinite-fringe mode for direct and quick phase visualization which may be required for certain problems of physical interest. The present paper describes a modification in the Llyod mirror interferometer in a manner, which permits direct phase visualization in infinite-fringe mode and as well can provide magnified phase information in finite-fringe mode, suitable to retrieve complete information. A grating has been used to form moiré pattern, which could generate both finite as well as infinite-mode information of the test object. The experimental results are in quite agreement with theory.

Keywords: Interferometry, Phase visualization, Moiré techniques

1. Introduction

Optical interferometric methods [1], which are non-contact, non-invasive, fast and most sensitive, have extensively been used for investigating transparent phase objects. Among these, interferometers where reference and test beams are derived from single optics [2-7] are considered are inherently stable, relatively insensitive to external vibrations and requiring fewer optical elements in contrast with conventional interferometry. Llyod mirror interferometer, which is in a category of one beam interferometer, some portion of a diverging beam strikes a front-surface mirror at a low angle and reflects off the mirror to a screen, and some portion of beam shines directly on the screen. The reflected beam forms a virtual second source that interferes with the direct beam. This generates a finite-fringe interferogram in the observation plane where varying that separation between the laser and the mirror changes the interference pattern on the screen. The phase shifting interferometry can be used to acquire a series of phase-shifted interferograms through a series of controllable phase delay steps to retrieve the information of the test object. It may be noted that the system has a limitation in that the deflection produced by the test object must not exceed the distance between the focal point and the folding mirror. This distance determines the initial fringe frequency to get complete information of the test object. If the mirror is placed too close to the focal point, light deflected towards the mirror will be obstructed by it's leading edge, resulting in a loss of phase information and also producing unwanted noise in the interferogram due to diffraction at the mirror edge. For this reason, the interferometer is more suited to the production of finite-fringe interferogram than near infinite-fringe interferogram. Thus, for the case where test object has randomly oriented or two directional index gradients, it becomes essential that the frequency must be quite high to ensure that deflected light should not be intercepted with the mirror's edge. The higher limit on the fringe frequency depends upon the resolution of the recording medium, where phase shifting techniques become somewhat erroneous [8]. Also, for problems of physical interest (e.g. flow visualization [9], on-line monitoring crystal growth [10] etc.) that requires direct phase visualization, it becomes very difficult to retrieve required information encoded in the fine finite-fringe interferograms. We present a

simple modification in the beam folding interferometer making it suitable either for direct phase visualization (infinite-fringe mode) or to provide complete and magnified phase information in finite-fringe mode. Here the position of the folding mirror is adjusted in such a manner that the initial fringe frequency becomes quite high to avoid interaction of deflected light from mirror's edge. A decoding grating with suitable spatial frequency is inserted at the location of interferometric fringes generating moiré patterns and by proper orienting the grating, moiré fringes running parallel to the interferometric fringes could be obtained. This finite mode moiré (having coarser spatial frequency) provides magnified information of the test objects particularly for study of index gradients producing right and left side or random deflections. Further, if position of grating is adjusted such that its spatial frequency matches to that with the spatial frequency of interferometric fringes, a single dark or light moiré fringe fills the field of view and the interferometer would provide infinite-fringe-mode information for direct phase visualization. Coarse finite-mode as well as infinite-mode moiré pattern could be used for acquiring complete and more accurate information using phase-shifting techniques [11, 12].

2. Theory

In two-beam interferometers, a pair of coherent light beams preferably derived from the same source of light is combined to create an interference pattern. The phase object is interposed in one of the beams called the test beam while the other beam is known as the reference beam. The interference pattern is of the form

$$h(x,y) = a(x,y) + b(x,y) \cos[2\pi\, f_o\, x + \phi(x,y)] \tag{1}$$

where $a(x,y)$ is a background intensity, $b(x,y)$ is the fringe or intensity modulation, f_o is a spatial carrier frequency and $\phi(x,y)$ is the phase function due to test object. Equation (1) generates a finite-fringe interferogram in the observation plane, where phase shifting interferometry of wavefront reconstruction is used to record a series of interferograms with a constant phase shift to get required information of the test object. Use of phase shifting technique, for the case of beam folding interferometer, has been nicely illustrated in reference [7]. Since the angle of deflected beam depends upon the direction of index gradients in the object, hence it becomes imperative to generate fine finite-fringes so as to accommodate both sided/directional information and also to avoid extra noise due to

diffraction. This is achieved simply by increasing distance 'a' in the well-known formula for fringe width in this geometry:

$$\beta = \lambda\, s/a \tag{2}$$

where s is the distance between the plane of the two point sources (focal point and its virtual image) and the observation plane and 'a' is the separation of two point sources (Fig. 1). It is obvious from Eq. (2) that theoretically there is no higher limit on the initial spatial frequency but experimentally the limit is decided by the resolution of recording material, where phase shifting techniques become erroneous. In order to overcome this problem, a grating of suitable spatial frequency acting as decoder is inserted at the location of interferometric fringes, as schematically shown in Fig. (2), facilitating in retrieving complete information of the test object.

The transmittance function of the sinusoidal grating, oriented at an angle θ with respect to the direction of interferometric fringes (Fig. 3) is expressed as:

$$t(x,y) = a_1(x,y) + b_1(x,y) \cos[2\pi\, f_1(x \cos\theta - y \sin\theta)] \tag{3}$$

where $a_1(x,y)$ and $b_1(x,y)$ are the constants specifying bias transmission and the modulation of the ruling and f_1 represents spatial frequency of the sinusoidal grating. Superposition of interferometric fringe pattern modulated by phase object with the grating yields [13]

$$I(x,y) = h(x,y) + t(x,y)$$

$$= a(x,y) + a_1(x,y) + b(x,y) \cos[2\pi\, f_o x + \phi(x,y)]$$

$$+ b_1(x,y) \cos[2\pi\, f_1(x \cos\theta - y \sin\theta)] \tag{4}$$

For simplicity, the contrast of both fringe patterns is assumed to be same (i.e. $a = a_1$ and $b = b_1$). Thus

$$I(x,y) = 2\, a(x,y) + 2\, a(x,y) \cos \pi\{x[\, f_o + f_1 \cos\theta] - y\, f_1 \sin\theta + \phi(x,y)\}.$$

$$\cos \pi\{\, x[f_o - f_1 \cos\theta] + y\, f_1 \sin\theta + \phi(x,y)\} \tag{5}$$

The first term in Eq. (5) is a dc term and the second term represents the moiré pattern with fringe width

$$D = (\beta d)/[\beta^2 + d^2 - 2\beta d \cos\theta]^{1/2} \tag{6}$$

with $\beta = 1/f_o$ and $d = 1/f_1$. This shows that the modulation of interferometric fringes due to phase object has been magnified by a factor $d/|\beta - d|$ due to pitch mismatch (i.e. $\theta = 0$) of the two periodic patterns. Here, it may be noted that similar phase magnification will also occur for angular mismatch,

but pitch mismatch moiré is more suitable in easy switching from finite to infinite mode patterns. The direction of moiré fringes with respect to y-axis in terms of angle of inclination Ψ is

$$\sin\Psi = d \sin\theta/\beta \tag{7}$$

This shows as the grating is aligned parallel to the interferometric fringes ($\theta = 0$), moiré fringes would also run parallel to these ($\Psi = 0$). This moiré pattern produces the similar results as available in conventional two-beam interferometry and the information about the first derivative of the phase distribution of the test object can be analysed. To adopt the phase-shifting techniques for the fringe analysis, one can write the moiré pattern fringe intensity distribution as

$$I(x,y) = 2\, a(x,y) + 2\, a(x,y) \cos \pi\{x[\, f_o + f_1] + \phi(x,y) + \delta(k_{21})\}.$$

$$\cos \pi\{ x[f_o - f_1] + \phi(x,y) + \delta(k_{21})\} \tag{8}$$

where, $\delta(k_{21})$ is the amount of phase shift. A transverse displacement of $|k_2 - k_1| = d/n$, ($n = 1, 2, 3, \ldots$) to the grating results in a phase change of $|\delta(k_{21})| = 2\pi/n$ for each fringe and phase profile can be obtained using well-known phase measurement techniques [12].

Equation (6) further shows that when the pitch of grating becomes equal to that of interferometric fringes ($\beta = d$) and the grating is aligned parallel to these ($\theta = 0$), width of moiré fringes (D) becomes infinite where a single dark (crossed position) or light (aligned position) moiré fringe would fill the field of view [14], modifying the Eq. (5) as:

$$I(x,y) = 2\, a(x,y) + 2\, a(x,y) \cos [2\pi\, f_o + \pi\phi(x,y)] \cos [\pi\phi(x,y)] \tag{9}$$

Equation (9) shows that the information of test object is associated with a noise term, which reduces contrast of resulting interferogram. This noise term could be removed by using spatial filtering technique to obtain a unit contrast infinite fringe mode information of test object whose intensity distribution at the observation plane is proportional to

$$I(x,y) \sim (1/2)a^2(x,y) [1 + \cos\phi(x,y)] \tag{10}$$

This infinite-fringe mode interferogram provides direct phase visualization of the test objects and could also be used for quantitative analysis using measurement techniques.

3. Experiment and results

The experimental arrangement is schematically shown in Fig. (2). A 35-mW He-Ne laser beam (6328-nm wavelength, Coherent 31-2140 model) is expanded and spatially filtered by using a 40 X microscope objective and a 5-μm pinhole. The diverging beam is collimated with a 400-mm focal length, f/4-collimating lens L_1 to generate 100-mm diameter collimated beam. A front surface silver coated plane mirror M (20mm X 40mm X 2mm; SiO_2 protected front surface silver coated; reflectivity ~ 94%) with its reflecting surface along the axis of the optical system is placed at a suitable distance from the axis to superimpose two halves of the same wavefront from lens L_2 (same specifications as L_1) to generate fine finite-fringe interferogram in the observation plane. A grating with a pitch of ~ 6 lines/mm is inserted at the location of the fringes and its position is adjusted to generate pitch mismatch moiré pattern with the interferometric fringe pattern. A phase shift of $\pi/2$ is introduced in the interferograms by providing ~ 42-μm (one-quarter of the grating pitch) in-plane displacement to the grating mounted on a precise translation stage (micro-control CV78 model). It may be noted that there is no stringent restriction on the pitch of the grating as the pitch of the interferometric fringe pattern varies with the distance from the plane mirror. For example, for source spacing 'a' of 1.5-mm, a grating of 6 lines/mm would be required at a distance 's' of 400-mm. Alternatively, the interferometric fringe patterns could be captured on a photographic plate and may be used as the requisite grating. The grating has accurate orientation when moiré fringes become parallel with the direction of the interferometric fringes and the pitch of two patterns matches when a single dark or light moiré fringe fills the field of view. The phase object to be studied is interposed in the test path, one half portion of the collimated beam, and the resulting interferogram is spatially filtered using a 200-mm focal length, f/4 lens, L_3 in conjunction with a 0.5-mm pinhole to get high contrast infinite mode information. The results presented have been captured frame-by-frame with a Canon S-50 Power Shot digital camera with 1024 x 768 pixel resolution and white balance settings.

Figure 4 presents typical test results of a glass plate having variable index gradients interposed in the conventional Llyod mirror interferometer using beam-folding technique. To accommodate this information, the position of mirror is brought further so as to generate fine fringes in the observation plane. However, it becomes difficult to visualize the phase object due to crowding of fringes. With the use of the grating and subsequent filtering as described above the information encoded in fine-fringes gets decoded. Figure 5 present the test results showing magnified information of the deflecting gradients in finite-fringe mode. Figure 6(a-c) depicts a series of phase-shifted interferograms (with a constant phase shift of $\pi/2$) of a portion of the test results shown, by giving suitable precise transverse displacement to the decoding grating. For direct phase visualization, finite mode moiré pattern is adjusted to an infinite-fringe mode and the test results obtained are shown in Fig. 7.

4. Discussion and Conclusions

A modification in the Llyod mirror interferometer has been reported for direct phase visualization. Use of pitch mismatch moiré pattern formed by superposition of interferometric fringes with a grating is described to obtain complete and magnified information of the test object.. Phase variation is achieved by an in-plane translation of the grating. Varying spatial frequency of the interferometric fringes further relaxes the stringent requirement on the spatial frequency of the grating. In our experiment, we used a binary grating but a sinusoidal grating is considered for mathematical simplicity. Generation of moiré fringes is quite helpful in easy and precise positioning of the grating with respect to the interferometric fringe pattern. Spatial filtering is applied to remove the unwanted noise and hence to improve contrast of resulting interferograms. The system is compact, easy to realize with basic optics components and quite stable to external vibrations as both the interfering beams are derived from the same collimating optics. However, proximity of reference and test beams makes the interferometer inappropriate for measurements where a large working room is required or in which surrounding is affected. The described system has a resemblance to zebra schlieren methods [15-17] and the Talbot interferometry [18, 19] where test object modulates images of zebra stripes or grating pattern while in our case test object modulates the fringe pattern itself, instead of its image, providing a better contrast. The method could further be extended to other conventional interferometers merely by using a converging lens and a grating.

References

[1] Malacara D (ed.) 1992 *Optical Shop Testing*, 2nd ed. (New York: John Wiley & Sons)

[2] Murthy M V R K 1964 The use of single plane parallel plate as a lateral shearing interferometer with a visible gas laser source *Applied Optics* 3, 531-534

[3] Smartt R N and Steel W H 1975 Theory and applications of the point diffraction interferometer *Japanese J Applied Physics* Supplementary 14-1 351-356

[4] Ferrari J A, Frins E M, Perciante D and Dubra 1999 A Robust one-beam interferometer with phase delay control *Optics Letters* 24, 1272-1274

[5] Aggarwal A K, Kaura S K, Chhachhia D P and Sharma A K 2005 A robust interferometer based on holographic optics *Experimental Techniques* 29, 21-24

[6] Raj Kumar, Kaura S K, Sharma A K, Chhachhia D P and Aggarwal A K 2007 Knife-edge diffraction pattern as an interference phenomenon: an experimental reality *Optics & Laser Technology* 39, 256-261

[7] Ferrari J A and Frins E M 2002 One-beam interferometer by beam folding *Applied Optics* 41, 5313-5316

[8] Gappinger R O, Greivenkamp J E and Borman C 2004 High-modulation camera for use with a non-null interferometer *Optical Engineering* 43, 689-696

[9] Aggarwal A K, Butuk N K, Gollahalli S R and Griffin D 1998 Three-dimensional rainbow schlieren tomography of a temperature field in gas flows *Applied Optics* 37, 479-485

[10] Srivastava A, Muralidhar K and Panigrahi P K 2005 Reconstruction of the concentration field around a growing KDP crystal with schlieren tomography *Applied Optics* 44, 5381-5392

[11] Greivenkamp J E and Burning J H 1992 Phase Shifting Interferometry in *Optical Shop Testing* Malacara D (ed.) 2nd ed. (New York: John Wiley & Sons) pp 501-598

[12] Robinson D W and Reid G T (ed) 1993 *Interferogram Analysis- Digital Fringe Pattern Measurement Techniques* (Bristol and Philadelphia: Institute of Physics Publishing) pp141-193

[13]   Sirohi R S and Chau F S 1999 *Optical methods of Measurement whole field techniques* (New York: Marcel Dekker) pp 227-274

[14]   Kaura S K, Chhachhia D P and Aggarwal A K 2006 Interferometric moiré pattern encoded security holograms *Journal of Optics A: Pure and Applied Optics* 8, 67-71

[15]   Peale R E and Summers P L 1996 Zebra schlieren optics for leak detection *Applied Optics* 35, 4518-4521

[16]   Massig J H 1999 Measurement of phase objects by simple means *Applied Optics* 38, 4103-4105

[17]   Settles G S August 9-12 2004 The Penn State Full-Scale Schlieren System *11th International Symposium on Flow Visualization, Notre Dame University, Indiana, USA*

[18]   Thakur M, Tay C J and Quan C 2005 Surface profiling of a transparent object by use of phase-shifting Talbot interferometry *Applied Optics* 44, 2541-2545

[19]   Garbusi E and Ferrari J A 2006 Defect enhancement in periodic masks using1/2 – Talbot effect *Optics Communications* 259, 55-59

List of Figure Captions

Figure 1 – Schematic representation of folding beam interference: F, point source (focus in our case); F', virtual image of F; M, folding mirror and OP, observation plane

Figure 2 – Schematic configuration of experimental setup; L, polarized He-Ne laser; SF, spatial filtering assembly; L_1, L_2, L_3 are lenses; O, phase object in test region; G, grating and F is the filter to remove noise from interferograms

Figure 3 – Geometry depicting formation of moiré fringes due to superposition of interferometric fringes with grating; θ is angle between y-axis and the grating lines; ψ is angle between y-axis and the moiré fringes; β, d and D are spatial frequencies of interferometric fringes, grating and moiré fringes respectively.

Figure 4 – Typical test results of a glass plate in fine interferometric fringes of Llyod mirror interferometer

Figure 5 – Test results of glass plate in modified Llyod mirror interferometer having

finite-fringe moiré pattern

Figure 6 – Three phase shifted interferograms with a constant phase shift of π/2 radians

of a portion of the test results typically shown by a square in Fig 5.

Figure 7 – Typical test results of glass plate in Llyod mirror interferometer having
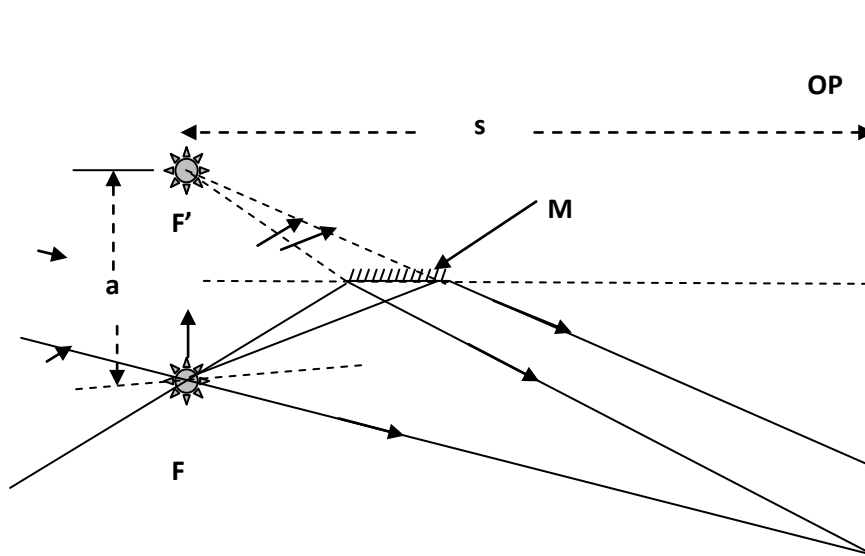
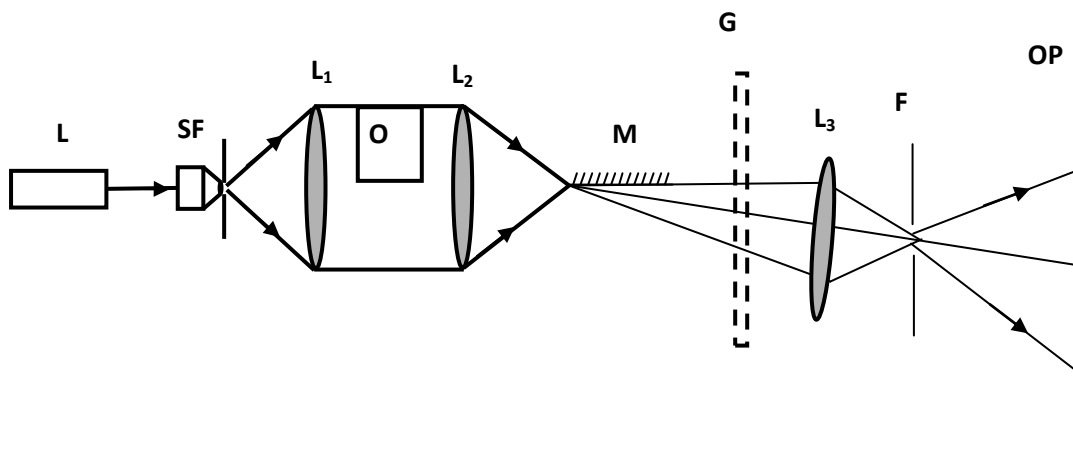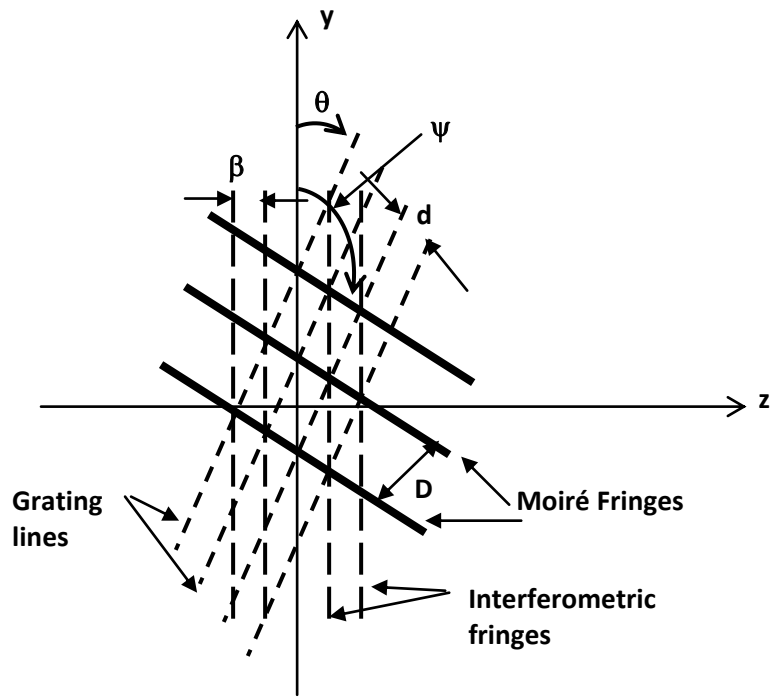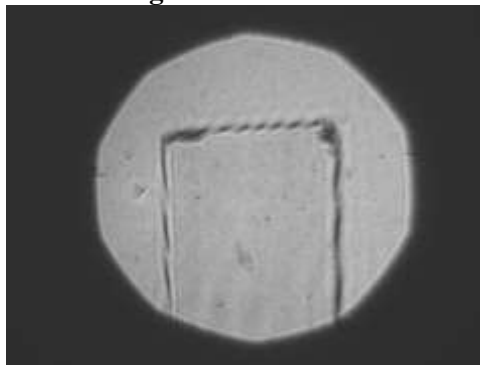infinite-fringe moiré pattern

Figure 1

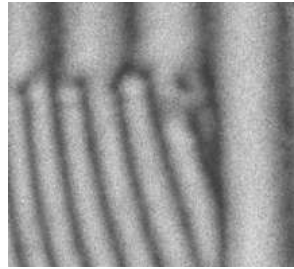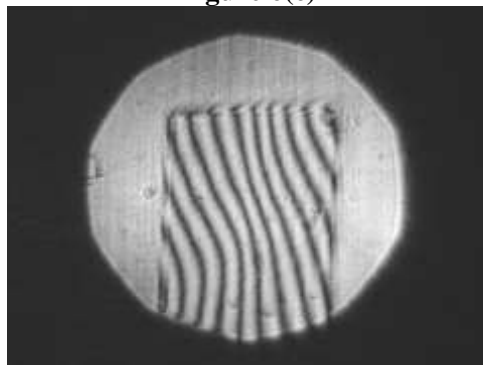**Figure 2**

Figure 3

Figure 4
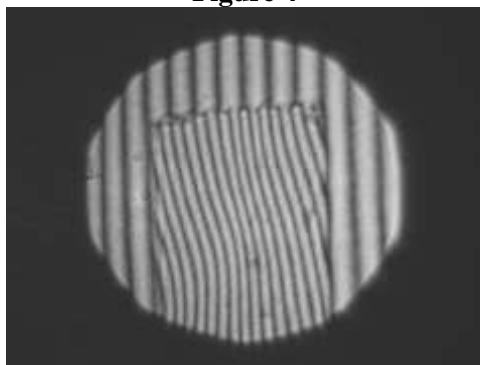
Figure 5
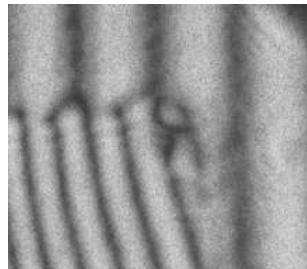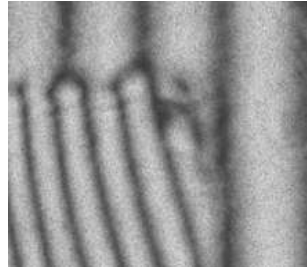
Figure 6(a)
Figure 6(b)
Figure 6(c)

Figure 7